Computer Assisted Mechanics and Engineering Sciences, 8: 513–526, 2001.

Numerical analysis of peristaltic blood flow in arteries[1]

Maciej Paszyński
Jagiellonian University, Department of Computer Science
ul. Nawojki 11, 30-072 Kraków, Poland

Andrzej Pelc
Jagiellonian University, Collegium Medicum
ul. św. Anny 12, 31-008 Kraków, Poland

(Received November 3, 1999)

The problem of blood flow in arteries induced by peristaltic waves has been investigated. The methodology of modelling global circulation system has been outlined. Medical measurements required for problem formulation have been presented. Numerical solutions of blood flow in artery based on finite element method have been worked out.

The paper presents local model of pulsatile blood flow in the human artery. Modelling of pulsatile flow in cardiovascular system could improve understanding and interpretation of flow measurements in arteries locally as well as ventricular–vascular interaction in healthy patients at rest and while exercising. Results achieved on local models could be generalized to formulate a global model of haemodynamics of cardiovascular system in man. This approach could help identifying physiology of optimal heart work at rest, physical activity and also in pathological conditions as hypertension, cardiac insufficiency, heart defects, coronary heart disease and origin and progression of artherosclerosis as well.

1. Motivation

Arterial part of cardiovascular system consists of the heart, aorta, arteries and arterioles and should be the subject of more precise modelling for diagnostic purposes. The main goal of this research is to formulate global model of pulsatile blood flow in central circulation system. A predicted clinical value of such a model is to facilitate matching therapeutical routines to particular clinical cases, more precise drug choice and administration and monitoring of rehabilitation results in cardiovascular system.

A global model is formulated by generalization results obtained from local 3D models, using input impedance function [20]. The most reliable local model, is concentrated on local 3 dimensional part of some artery, and should contain a few parts assembled together:

- peristaltic blood flow model, maintaining the blood flow in local 3-dimensional part of some artery,
- arterial wall dynamics model,
- interactions flow–arterial wall distension model, very similar to dynamical fluid–solid interaction problem.
- pulse wave reflection at arteriolar level.

[1]The paper has been presented at the XIVth Polish Conference on Computer Methods in Mechanics, PCCMM'99, Rzeszów, May 26–29, 1999.

As may be seen from the above, blood flow in central circulation system has very compound pulsatile character. Heart works in cycles and arterial response is cyclic too. Wave reflection is so timed as to return to the ascending aorta from the periphery when the heart muscle is relaxed, and so as to boost the pressure perfusing the coronary arteries. Such a situation is highly advantageous [19]. Efficiency of such a system depends on very sensitive physical phenomenon such as cyclic shift of reflected pulse wave.

The paper presents the results of the research carried out into above mentioned peristaltic blood flow model, maintaining blood flow in local 3 dimensional part of some artery. A local flow model assuming constant shape of peristaltic wave propagation without feedback has been investigated. It is not possible to fully understand assumptions of such a model without introducing anatomy and physiological principles of central circulation system, as well as interactions between hydrodynamical system and artery's wall dynamic system described below in detail.

Usually flow of blood in arteries is established to be non-Newtonian, viscoelastic and thixotropic. The most popular description is a Casson model described in [28]. The peristaltic blood flow was represented by two layers of axisymmetric 3D fluid model in cylindrical coordinates system, where the core region with erythrocytes was assumed to be Casson fluid and peripheral plasma region was established as Newtonian fluid. Analytical results presented in [28] assume that there is a zero radial pressure gradient and the problem is axial symmetrical. Excluding walls distension, such a model does not allow us to describe process of energetic exchanges resulting from potential energy of pressure gradient elasticity of walls. The energy exchange process plays the crucial role as the base of peristaltic transport. Variational formulations of analytical models formulated in cylindrical coordinate system can also be singular. Another disadvantage of that model is that information about the locations of surface which separate different kinds of flows are necessary. It makes that model impractical.

A 3D model involving non-zero radial pressure gradient and non-axially symmetrical velocity field should be applied. Arteries are large vessels and flow velocity is so high, that it is reasonable to describe such blood flow as Newtonian fluid case [20]. Casson model seems to be suitable for describing peristaltic blood flow in capillaries where radial pressure gradient is negligible.

2. Definition of the peristaltic blood flow

According to [26, 27] the peristaltic transport may be explained as the mechanism by which fluid can be transported through distensible tube when contraction or expansion waves propagate progressively along its length. In the human body peristalsis is the primary physiological mechanism used to move fluids from one place to another (Such as ureter, male reproductive system, gastro-intestinal tract, bile duct). Latham [14] was probably the first to investigate the mechanism of peristalsis in relation to mechanical pumping. In the case of blood flow in central circulatory system, there are two components: pulsatile and subsequent peristaltic. Pulsatile component appears because the heart perform cyclic pumping. The peristaltic blood flow component results from propagation of expansion wave and pressure gradient, along the arterial wall, arised from blood eruption from the heart. This phenomenon could be divided into two parts. The first, propagation of wave along the elastic wall, and the second, the mass transport with much lower velocity.

3. Characteristics of human cardiovascular system

The cardiovascular system is composed of the heart, conduit arteries, small arteries, capillaries and veins. The vessel wall itself is composed of elastic fibers and smooth muscle fibers, see [16]. Arterial wall is able to withstand blood pressure with passive tension of elastic fibers and active contraction of smooth muscles.

3.1. Anatomy and distinguishing of modelling domain

Functional classification (see Fig. 1)

The blood vessels, together with four chambers of the heart form a closed system for the flow of blood; only if there is an injury to some part of the wall of this system does any blood escape. Arteries carry blood from the ventricles (pumping chambers) of the heart out to the capillaries in organs and tissues. The smallest arteries are called arterioles.

Arteries are distensible, low-resistance tubes conducting blood to the various organs with little loss in pressure. They act as pressure reservoirs for maintaining blood flow during ventricular relaxation. The arterioles are the major sites of resistance to flow, and are responsible for the pattern of blood flow distribution to the various organs. Linear velocity of blood in arteries is about 20–100 cm/s.

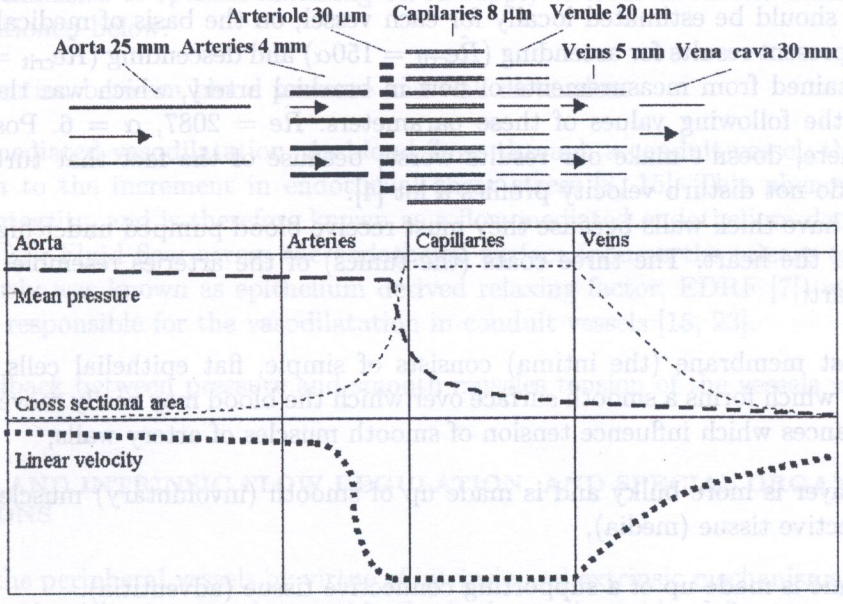

Fig. 1. Arterial components of circulatory system

The investigation of the problem of the transition from laminar to turbulent flow in arteries is uniquely difficult, partly because the unsteady nature of the basic flow renders disturbances and partly because of limitations of instrumentation and access [17]. In the case of steady flow, the laminar structure of flow is confined by the critical Reynolds number, above which the structure of flow becomes turbulent.

Reynolds number $Re = \frac{\varrho UD}{\eta}$ (ϱ – density of a fluid, U – mean velocity, η – fluid viscosity, D – diameter of a fluid) expresses the proportion of inertial force to friction force [20]. Hence [18] it is expected that turbulence might occur in larger arteries during systole. The cited investigations show that diastole was a quiescent period, and the disturbances in the descending aorta appear not to have been convected from the heart but locally generated.

It was thus of interest to attempt defining the origin of the turbulence, in the sense of distinguishing between free-stream turbulence existing in the blood ejected from the ventricle, and local flow disturbances in aorta [18].

It was presumed that two sources of turbulances exist: (1) flow disturbances originating in the ventricle as origin of turbulence, (2) disturbances in the descending aorta which have not been convected from the heart but locally generated.

Assuming blunt velocity profiles it was found that blood ejected from the heart reaches arch region during one beat and penetrates the descending aorta on the second beat. After isoprenaline administration, turbulences augments in descending aorta, however, blood is in its second pulse

since being ejected from the heart, and had already undergone a quiescent diastolic period. This observation points out that flow disturbances was not originated by heart ejection but was generated locally within descending aorta.

It was noticed that for pulsatile flow the Re number is not the accurate parameter for prediction turbulence to develop. That is why parameter α was introduced, which takes into account also the heart rate and viscous forces. It was observed [24] that turbulences were only occasional phenomenon which was found only in smaller animals. These observations suggests that the α parameter should be proportional to both vessel size and heart rate. According to [17], the parameter α is defined as $\alpha = R\sqrt{\frac{\omega\varrho}{\eta}}$ ($\omega = 2\Pi f$, f – heart rate, R – vessel radius).

Both α parameter and Reynolds number for pulsatile flow, defined as $\hat{R}e = \frac{\hat{U}\varrho}{\eta}$ (where $\hat{U}$ denotes peak velocity) seems to be accurate to calculate criteria for laminar and turbulent pattern of pulsatile flow [17, 18]. Critical Reynolds value $\hat{R}e_{\text{crit}}$ is a function of α parameter ($\hat{R}e_{\text{crit}} = \text{const} \cdot \alpha$). Constant value should be estimated locally for each vessel, on the basis of medical measurements. Papers [17, 18] present results for ascending ($\hat{R}e_{\text{crit}} = 150\alpha$) and descending ($\hat{R}e_{\text{crit}} = 250\alpha$) thoracic aorta. Data obtained from measurements of flow in brachial artery, which was the subject of our study, suggest the following values of these parameters: $\hat{R}e = 2087$, $\alpha = 6$. Possible appearing of turbulence here, doesn't make our results worse, because of the fact that turbulence has low amplitude and do not disturb velocity profiles a lot [4].

The arteries have thick walls because they must receive blood pumped under high pressure from the ventricles of the heart. The three coats (the tunics) of the arteries resemble the three tissue layers of the heart:

- the innermost membrane (the intima) consists of simple, flat epithelial cells making up the endothelium which forms a smooth surface over which the blood may easily move. It also secretes active substances which influence tension of smooth muscles of artery walls,
- the second layer is more bulky and is made up of smooth (involuntary) muscle combined with elastic connective tissue (media),
- the outer tunic is made up of a supporting connective tissue (adventitia).

The largest artery, the aorta, is about 2.5 cm (1 inch) in diameter and has the thickest wall because it receives blood under high pressure from the left ventricle. The smallest subdivisions of arteries, the arterioles, have thinner walls in which there is very little elastic connective tissue but relatively more smooth muscle.

Capillaries are the smallest vessels. The microscopic branches of these tiny connecting vessels have the thinnest walls of any vessels, they consist of only one cell layer. The capillary walls are transparent and are made of smooth, plate like cells that continue from the lining of the arteries. Because of the thinnes of these walls, exchanges between the blood and the body cells are possible. The capillary boundaries are the most important center of activity for the entire circulatory system.

3.2. Physiology

It must be emphasized again that the output of the heart is pulsatile, and the response of the arterial tree is pulsatile too. The tubular design of the arterial system, its branching network and its termination in arterioles result in generation of waves which pass to the periphery along low-resistance pathways, then are reflected at the junction of the low resistance pathways with high resistance arterioles [19, 21].

The same vascular properties that cause mean arterial pressure to fall only slightly over one meter or more, and then to drop precipitously over several millimeters, also cause pulsatile components of pressure to be reflected and return in retrograde fashion to the heart. The pressure (or flow) wave

recorded in any artery is a combination of an impulse travelling forward from the heart together with components travelling back towards the heart [19].

Cardiac output is 5 l/min at rest and 30 l/min while exercising. It gives the average flow from 7200 l/24h to about 50000 l/24h. Human heart works on average 70 years. From this point it's clearly visible that optimizing of energy expenditure is important, that is why blood flow in human arteries is pulsatile. Intermittent pumping enables only 10% of energy to be utilized in steady pumping. Therefore, pulsation of flow makes the heart work ten times more efficient.

At the beginning of each pulse of flow there is a flat profile of linear velocity so as to avoid dissipation of energy caused by friction of fluid layers, at the end the profile is similar to parabolic. Pulsatile flow is also more resistant to turbulence in spite of Reynolds number above critical value.

Any disturbances of the cardiovascular system that change flow profile or parameters of heart work lead to development of premature cardiac insufficiency.

There are mechanisms of optimal matching blood supply to local metabolic demand. Only three of them are mentioned below.

- Passive interaction between blood pressure and wall distension.
- Active flow mediated vasodilatation. As blood flows through a conduit vessel, the vessel dilates in proportion to the increment in endothelial shear stress [8, 15]. This phenomenon requires endothelial integrity, and is therefore known as a flow-mediated endothelium-dependent vasodilatation [10, 22]. Fluid flow across the endothelial surface induces the release of EDRF (nitric oxide previously was known as epithelium derived relaxing factor, EDRF [7]) which is thought to be largely responsible for the vasodilatation in conduit vessels [15, 23].
- Negative feedback between pressure and smooth muscles tension of the vessels walls.

4. EXTRINSIC AND INTRINSIC FLOW REGULATION, AND SPECIAL ORGAN CIRCULATIONS

Dual control of the peripheral vessels by virtue of intrinsic and extrinsic mechanisms makes possible a number of vascular adjustments that enable the body to direct blood flow to areas where it is needed in greater supply and away from areas whose immediate requirements are smaller.

In the brain and the heart, vital structures with a very limited tolerance to a reduced blood supply, intrinsic flow-regulating mechanisms are dominant. For instance, sudden fall of blood volume as might occur in severe acute hemorrhage, has negligible effects on the cerebral and cardiac resistance vessels whereas skin, renal, and splanchnic blood vessels become greatly constricted.

In skeletal muscle the interaction and changing balance between extrinsic and intrinsic mechanisms can be clearly seen. In resting skeletal muscle, neural control (vasoconstrictor tone) is dominant, as can be demonstrated by large increment in blood flow that occurs immediately after section of the sympathetic nerves to the tissue. In anticipation of and at the start of exercise, such as running,

Table 1. Distribution of the systemic cardiac output at rest and during exercise

	rest (ml/min)	Strenuous exercise (ml/min)
Brain	750	750
Heart	250	750
Muscle	1200	12500
Skin	500	1900
Kidney	1100	600
Abdominal Organs	1400	600
Other	600	400
Total	5800	17500

there is an increase in blood flow in the leg muscles, possibly mediated by activation of the cholinergic sympathetic dilatator system (Table 1). After the onset of exercise the intrinsic flow-regulating mechanism assumes control, and because of the local increase in metabolites, vasodilatation occurs in the active muscles. Vasoconstriction occurs in the inactive tissues as a manifestation of general sympathetic discharge, but constrictor impulses reaching the resistance vessels of the active muscles are overridden by the local metabolic effect [3].

5. Aim of modelling tool of precise diagnostics

There are three main pathologies of cardiovascular system (see Figs. 2 and 3 [9, 13]).

- Arterial hypertension.
- Cardiac insufficiency.
- Valvular defects.

As it is clearly seen, these pathologies affects a significant part of the population.

Generally, we may consider three models connected to each other: *conceptual model*, *local physical model*, *diagnostic model*.

By analogy with the theory of non direct current schemes, blood flow in central circulation system may be compared with current flow in RLC schemes [20]. Each part of circulation system (particular arteries) may be represented as RLC scheme. Then, these parts are joined together into

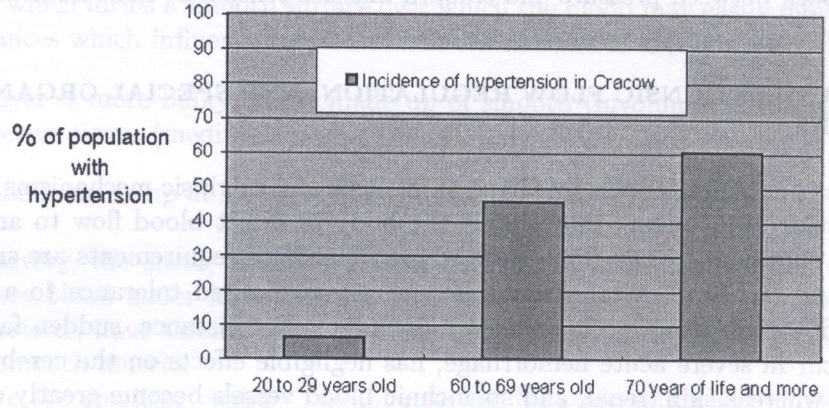

Fig. 2. Incidence of hypertension in Cracow [13]

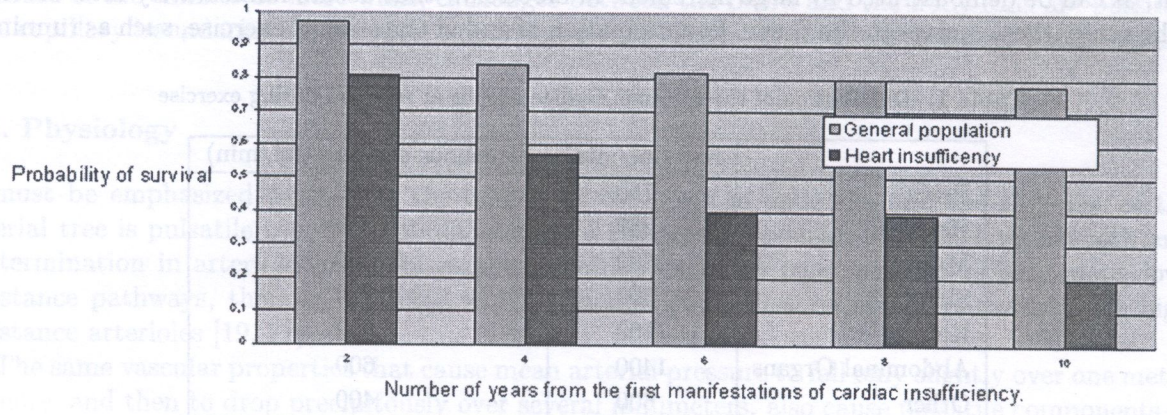

Fig. 3. Cardiac insufficiency [9]

a virtual scheme of central circulation system. Such virtual model, fast applicable in real time, is called *the conceptual model.*

To create conceptual model, it is necessary to identify RLC parameters describing each part of central circulation system. It may be performed on the basis of medical measurements, and numerical modelling of blood flow in interaction with vessel wall, based on Navier–Stokes equation. Such a numerical model, used for blood flow simulating in particular arteries is called *the local physical model.* The paper presents preliminary local physical model, without flow-arterial wall interactions.

Local physical models may be useful for verifying the conceptual model, by calculating RLC parameters identifying particular parts of the central circulation system. It is intended to create *the diagnostic model,* artificial intelligence for clinical use, based on inverse solution (parameters identification) of conceptual model.

Modelling of pulsatile flow in the cardiovascular system could give a better understanding of physiology of optimal heart work, could help in matching therapeutical procedures in particular cases and to establish more accurate prognosis. Recent progress in the development of non invasive methods enabled higher accuracy in obtaining measurements related to blood flow which in term allowed development and validation of local physical models and conceptual model as well.

6. THE MODEL OF PERISTALTIC BLOOD FLOW IN SOME PART OF ARTERY

Let us consider the model of peristaltic blood flow in some part of the artery. With respect to the chronology mentioned in chapter *Motivation*, the model should be understood as peristaltic blood flow model, constitute a part of local 3D model, describing local part of some artery. With respect to the chronology mentioned in chapter *Aim of modelling tool of precise diagnostics*, the model should be understood as 3D local physical model.

This model concerns part of the artery, which walls are deformed with peristaltic wave understood as pulse pressure wave (Fig. 4). Above defined deformation propagates along the artery and could be identified with pulse wave. There are two coordinates systems used for the problem description. First, stationary, dimensional, is the main coordinates system, fixed to the tube, and connected with laboratory point of view (axes X_1 , X_2 , X_3, variables denoted by capital letters). Second, dimensional coordinates system moving with peristaltic wave (axes x_1 , x_2 , x_3, variables denoted by small letters). Consider long uniform tube, filled with fluid, and the tube deformation, constant in shape, shifted along to tube longitudinal axis, with constant velocity. From moving with deformation coordinates system point of view, under above conditions, the flow problem may be considered to be stationary, simple and easy to formulate and solve. That is why the model is formulated in coordinates system moving with peristaltic wave. The modelling area, denoted by Ω, is defined as a finite-length arterial part, limited by a range of deformation performed by peristaltic wave.

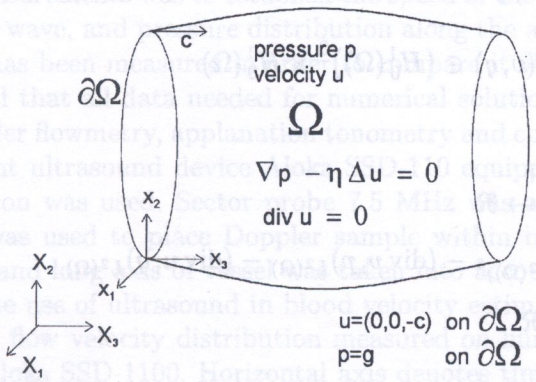

Fig. 4. Peristaltic blood flow in artery

Area Ω is defined in coordinates system moving with pressure wave. The beginning of the moving coordinates system is pinned into the left-bottom point of the area (see Fig. 4). The area Ω with its coordinates system is moving with pressure wave along the artery. Boundary velocity is constant and equal to minus propagation speed in moving coordinates system. The boundary pressure distribution does not depend on time, either.

The Newtonian model (see [6]) $\sigma^i_j = -p\delta^i_j + 2\eta V^i_j$ $(i,j = 1,2,3$, σ^i_j – stress tensor, V^i_j – strain-rate tensor, p – hydrostatic pressure, δ^i_j – Kronecker delta, η – viscosity coefficient) implies the Stokes equations formulated in 3D Cartesian coordinates system,

$$\nabla p - \eta \Delta u = 0, \tag{1}$$

$$\operatorname{div} u = 0, \tag{2}$$

satisfied in Ω. The boundary conditions satisfied on $\partial\Omega$ are

$$u = b, \qquad p = g, \tag{3}$$

where g is a given boundary pressure distribution, $b = (0,0,-c)$ where c is the peristaltic wave propagation speed. The boundary condition is no-slip condition on the wall. Arterial wall, standing in fixed coordinates system, from peristaltic wave point of view, is moving in the contrary direction with the propagation speed. If the wall velocity is $-c$, it is obvious that boundary fluid layer velocity is also $-c$. Differentiation here is understood in weak variational sense.

Homogenous boundary value Stokes problem in Cartesian coordinates system is obtained after suitable shift,

$$\hat{u} = u - \bar{u}, \qquad \hat{p} = p - \bar{p}, \tag{4}$$

where $(\bar{u},\bar{p}) \in \left(H^1(\Omega)\right)^3 \times H^1(\Omega)$ established, such that $\operatorname{tr}\bar{u} = b$ on $\partial\Omega$ (for example $\bar{u} \equiv b$ is satisfying this condition), $\operatorname{tr}\bar{p} = g$ on $\partial\Omega$. Trace tr here is understood as weak variational restriction onto the boundary $\partial\Omega$. Homogenous boundary value Stokes problem consists in finding $(\hat{u},\hat{p}) \in \left(H^1_0(\Omega)\right)^3 \times H^1_0(\Omega)$ which satisfy

$$\nabla\hat{p} - \eta\Delta\hat{u} = f, \qquad \text{on } \Omega, \tag{5}$$

$$\hat{u} = 0, \qquad \text{on } \Omega, \tag{6}$$

$$\hat{u} = 0, \quad \hat{p} = 0 \qquad \text{on } \partial\Omega, \tag{7}$$

where $f = -\nabla\bar{p}$ is a given right-side vector.

We will use another form of this equations, more suitable for performing numerical calculations. After dropping hats over $\hat{u}$ and $\hat{p}$ we obtain

$$a(u,p;v,q) = f(v,q) \qquad \forall (v,q) \in \left(H^1_0(\Omega)\right)^3 \times H^1_0(\Omega) \tag{8}$$

where

$$a : \left(\left(H^1_0(\Omega)\right)^3 \times H^1_0(\Omega)\right)^2 \mapsto \Re \tag{9}$$

$$a(u,p;v,q) = \eta(\nabla u, \nabla v)_{(L^2(\Omega))^3} - (\operatorname{div} v, p)_{L^2(\Omega)} - (\operatorname{div} u, q)_{L^2(\Omega)}, \tag{10}$$

$$f : \left(H^1_0(\Omega)\right)^3 \times H^1_0(\Omega) \mapsto \Re \tag{11}$$

$$f(v,q) = \eta(f,v)_{(L^2(\Omega))^3}. \tag{12}$$

We refer to the book [29] for the existence and uniqueness.

7. Hughes–Franc method

The Stokes problem belongs to the class of saddle-point problems for which an abstract theory has been developed [1, 2]. The theory shows that the method is optimally convergent if the finite element spaces for velocity and pressure satisfy the Babuška–Brezzi or inf–sup condition. In computations the violation of this condition often leads to unphysical pressure oscillations and locking of the velocity field [11]. The Hughes–Franc method, a recent technique of stabilizing mixed method has been used for improving stabilization of numerical solution.

We restrict our considerations to 3D tetrahedral Lagrangian elements. We introduce the following finite element spaces

$$P_m = \left\{ p(x): \quad p(x) = \sum_{|\alpha| \le m} a_{\alpha_1 \alpha_2 \alpha_3} x_1^{\alpha_1} x_2^{\alpha_2} x_3^{\alpha_3} \right\} \tag{13}$$

$$V_h = \left\{ v \in \left(H_0^1(\Omega)\right)^3 : \quad v_i \,|_K \in P_m(K) \quad \forall K \in T_h \right\} \tag{14}$$

$$P_h = \left\{ p \in L_0^2(\Omega) : \quad p \,|_K \in P_l(K) \quad \forall K \in T_h \right\} \tag{15}$$

Hughes–Franc method consists in finding a pair $(u_h\,,\, p_h) \in V_h \times P_h$ such that

$$B(u_h\,,\, p_h; v, q) = F(v, q) \quad \forall (v, q) \in V_h \times P_h \tag{16}$$

where

$$B : (V_h \times P_h)^2 \mapsto \Re \tag{17}$$

$$B(u_h\,,\, p_h\,;\, v,\, q) = a(u_h\,,\, p_h\,;\, v,\, q) - \alpha \sum_{K \in T_h} h_K^2 \left(-\eta \Delta u_h + \nabla p_h\,,\, -\eta \Delta v + \nabla q\right)_K\,, \tag{18}$$

$$F : V_h \times P_h \mapsto \Re \tag{19}$$

$$F(v, q) = f(v, q) - \alpha \sum_{K \in T_h} h_K^2 \left(f\,,\, -\eta \Delta v + \nabla q\right)_K\,, \tag{20}$$

$(\,,\,)_K$ denotes the scalar product over element K, $h_K = \mathrm{diam}(K)$ denotes the diameter of element K, $\alpha \in \Re$ is some parameter.

For improving stabilization the standard Galerkin form is modified by the addition of mesh-dependent terms which are weighted residuals of the differential equations.

8. Medical measurements

Medical measurements have been made in the case of the peristaltic blood flow in human brachial artery. The aim of that measurements was to establish the speed of the peristaltic wave propagation, the shape of the peristaltic wave, and pressure distribution along the artery interval. Also the blood flow velocity distribution has been measured in order to compare it with simulation results.

It should be emphasized that all data needed for numerical solutions could be obtained by non invasive technique as Doppler flowmetry, applanation tonometry and cuff manometry (Figs. 5 and 6).

For clinical measurement ultrasound device Aloka SSD-110 equipped with pulsed wave system for blood velocity estimation was used. Sector probe 7.5 MHz was applied on the brachium skin and duplex presentation was used to place Doppler sample within brachial artery and the angle between ultrasound beam and long axis of vessel was taken into account while velocity estimation. More information about the use of ultrasound in blood velocity estimation can be found in [12].

Figure 5 presents blood flow velocity distribution measured on human brachial artery by using ultrasonographic station Aloka SSD-1100. Horizontal axis denotes time, vertical axis denotes components of the velocity distribution. It follows that axial velocity amounts to 181 cm/s. This velocity is induced by peristaltic wave propagation accompanying blood eruption by the heart.

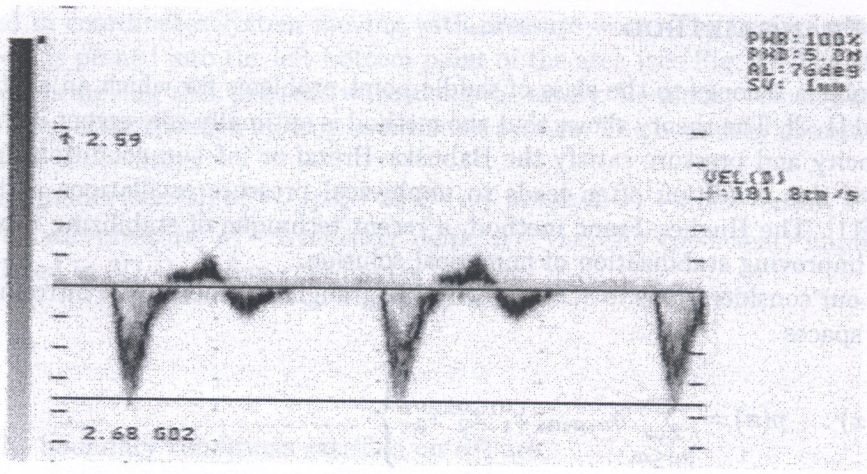

Fig. 5. Blood flow velocity distribution measurement

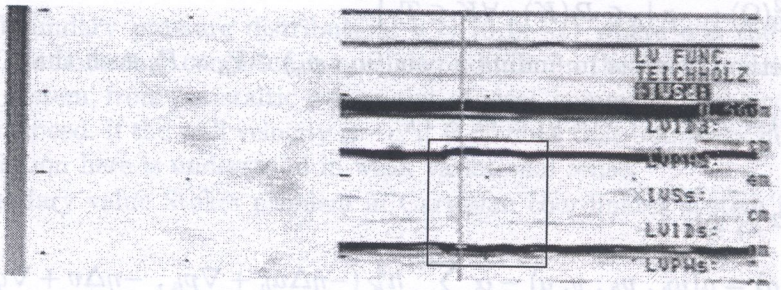

Fig. 6. Peristaltic wave shape measurement

Figure 6 presents peristaltic wave shape measurements also made by using ultrasonographic station Aloka SD-1100. On the left side of the picture there is an ultrasonographic view of the human brachial artery. The artery is directed perpendicular to the picture area. On the right side there is a sequence of snap-shots presenting the artery cross-sections made in regular time intervals. The peristaltic wave shoulder is denoted by a square. Since the length of time interval is equal to 0.281 s, and a peristaltic wave propagation speed has been established (as averaged value) as 200 cm/s, it follows that the length of this shape is about 60 cm ($s = V \cdot dt \Rightarrow 200 \cdot 0.281 = 56.2$ cm). The diameter of the artery has been established as 0.6–0.7 cm.

With regard to measurements mentioned above, the shape of elementary blood vessel (called domain of solution and denoted by Ω) has been established as 60 cm on 0.6 cm. It should be emphasized that the shape of Ω has been measured on the one established section of artery. It means, that the Ω denotes the section of artery changes in time induced by pressure wave. The peristaltic wave propagation speed has been established as 2 m/s (see Fig. 7). The bounded regular domain of solution $\Omega \in \Re^3$ has been divided into a finite family T_h of 3D Lagrangian elements $K \in T_h$.

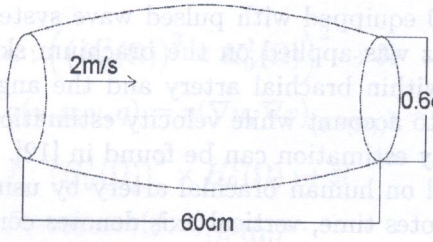

Fig. 7. The domain of solution

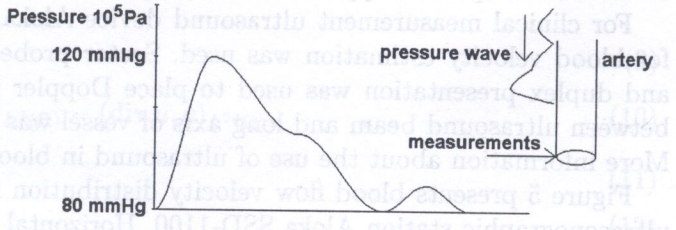

Fig. 8. Pressure boundary values

Pressure boundary values distribution presented in Fig. 8 has been established on the basis of applanation tonometry and cuff manometry measurements. The shape of pressure average values graph has been obtained from applanation tonometry measurements. Minimum and maximum pressure values have been measured by using traditional cuff manometry.

Blood viscosity has been assumed to be constant and equal $\eta = 4 \cdot 10^{-3}$ kg m^{-1}s^{-1} [20]. This value is typical for blood flow in arteries in healthy man under standard conditions.

9. Results of simulation

Implementation of the application which performs Hughes–Franc method consists of the following parts: mesh generation, stiffness matrix and right-hand-side vector parallel calculation, parallel GMRES solving linear system, results visualization.

The implementation is non-homogeneous, regarding architectural properties and programming paradigms as well as the basic programming tools to be used. Mesh generation is implemented using traditional procedural C++ programming. The key FEM parts of application performing mesh generation and calculation of data structures of a discrete algebraic system, as well as the discrete linear system solution are purely object-oriented.

The mesh generator described in details in [5] divides bounded regular domain of solution into flat levels, and attempts to triangulate the first layer by using algorithm of 2D Delunay triangulation. Then this triangulation is copied into remaining layers, and next, with the use of nodal points from two consecutive layers basic cells of triangulation are built. Each of these cells is spread to six simplexes of cubic triangulation in a canonical way. If necessary, the initial mesh is transformed into non-cylindrical mesh. Mesh nodes take new position, but triangulation topology remains unchanged. Also, if needed, the generator is dividing the achieved mesh into several subdomains suitable for parallel computation.

The methodology of designing and creating an open distributed CAD systems described in [25] was utilized by parallel stiffness matrix and right-hand-side vector calculations.

The parallel distributed solver based on GMRES (generalized minimum residual) algorithm [5] was used to solve the obtained linear system. Mesh generator was written in C++ by using traditional paradigm of procedural programming. Finite element method and linear solver were written in C++.

Results presented in Figs. 9, 10 has been achieved by using Hughes–Franc method with piecewise linear approximations of velocity and pressure.

Calculations have been performed inside the area denoted by Ω, which constitute a part of the artery being deformed by peristaltic wave (understood as pulse pressure wave), propagated along an artery wall. The area Ω (as it was described in chapter *The model of peristaltic blood flow in some part of artery*) is moving with peristaltic wave along an artery. Pressure values diagram on the boundary of the moving area Ω has been drawn by attaching measuring device at one established

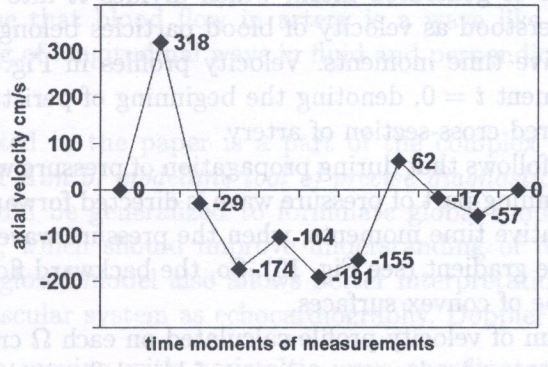

Fig. 9. Maximum of axial velocities calculated on cross-sections of peristaltic wave tube

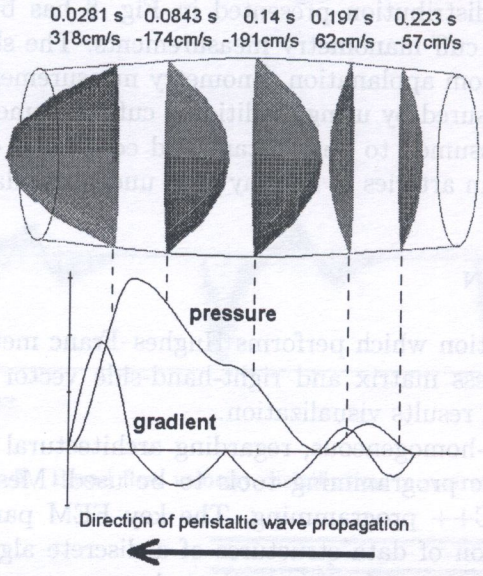

Fig. 10. Pressure boundary values obtained from measurement, calculated pressure gradient, velocity profiles calculated by using Hughes–Franc method

point of artery boundary. Then, propagating pressure wave has been recorded (see Fig. 8). X-axis has two meanings. First, it denotes time axis (time of the whole propagating pressure wave was measured as 0.281 s). Second, X-axis also denotes distance from the beginning of deformed area Ω, moving with pressure wave (because the speed of pressure wave was equal to $200cm/s$, the length of deformed area Ω was about 56.2 cm $= 0.281 \cdot 200$ cm). This is no wonder because it is a wave-like phenomenon, and pulse wave propagates in time and space, as it is denoted in classic wave equation.

Velocity vector field and pressure scalar field on Ω have been calculated by using Hughes–Franc method. Calculated pressure field presents little fluctuations of boundary pressure values. Calculated velocity field is presented in Figs. 9, 10. The velocity field is presented in fixed coordinates system, not moving with pressure wave. Points on X-axis denote time moments of simulated velocity profiles, performed at one established cross-section of artery, along which pressure wave is propagated. When in fixed coordinates system we focus on one cross-section of artery, along which the pressure wave is propagated, and calculate velocity profiles at the successive time moments, then we achieve (see Fig. 10) the following velocity profiles of blood particles of the established cross-section. The area Ω with its coordinates system, as it was described above, is moving with pressure wave along to artery. X-axis may also be understood as X-axis of moving coordinates system. Then, velocity profiles may be understood as calculated for successive cross-sections of the area Ω.

Each velocity profile presented in Fig. 10 has been drawn by connecting (by convex surface) ends of velocity vectors pinned on artery cross-sections. Velocity vectors has been calculated by finite elements method at vertexes of generated mesh, which divides Ω into cross-sections. Calculated velocity profiles may be understood as velocity of blood particles belonging to one cross-section of artery, calculated in successive time moments. Velocity profiles in Fig. 10 have been indexed by time distance from time moment $t = 0$, denoting the beginning of peristaltic wave (pressure wave) propagation through considered cross-section of artery.

From calculated results it follows that during propagation of pressure wave on one cross-section of artery, blood flow at the beginning part of pressure wave is directed forward, and achieves maximum velocity value. In the consecutive time moments, when the pressure wave is propagated, the flow is directed according to pressure gradient (see Fig. 10). So, the backward flow is also present. Velocity profiles have always the shape of convex surfaces.

Figure 9 presents maximum of velocity profile calculated on each Ω cross-sections. The shape of obtained diagram is similar to medical measurements of blood flow velocity on established cross-section of artery, during propagation of pressure wave (compare with Fig. 5). Only one difference

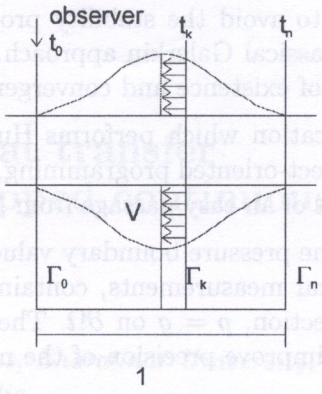

Fig. 11. Flow balancing in moving coordinates system

is that medical measurements have used reversed coordinates system. Calculations performed by using other boundary pressure values shows that the problem is very sensitive on prescribed pressure boundary distribution.

One can say that the traditional form of the law of continuity is not satisfied. There is a special way of flow balancing, because the problem has been solved in coordinates system that follows the peristaltic wave (see Fig. 11)

The peristaltic wave deformation is displaced relatively to the fixed observer position. The volume of this deformation must be equal to the total discharge of the peristaltic wave. It can be calculated as the following integral,

$$V = \int_{t_0}^{t_K} \left(\int_\Gamma u \, \mathrm{d}\sigma \right) \mathrm{d}t. \tag{21}$$

The integral may be approximated in the following way,

$$V \cong \sum_{i=1}^{n} \Delta t \left(\int_\Gamma u \left(t_i + \frac{\Delta t}{2} \right) \mathrm{d}\sigma \right), \tag{22}$$

$$\Delta t = \frac{\Delta l}{c} = \frac{l}{nc} \quad \Rightarrow \quad V \cong \sum_{i=1}^{n} \frac{l}{nc} \left(\int_\Gamma u \, \mathrm{d}\sigma \right). \tag{23}$$

The elliptic type of Stokes equations forces the flow direction to be coherent with direction of the pressure gradient. When there is a positive pressure gradient in the assumed moving coordinates system, the flow is directed contrary to peristaltic wave propagation, and when there is a negative pressure gradient, the flow is directed according to the propagation (see Fig. 10).

10. Conclusions

- Obtained results disclose that blood flow in artery is a wave like phenomenon and could be interpreted as assembling of longitudinal wave in fluid and perpendicular wave on the vessel wall (Fig. 10)
- The local model presented in the paper is a part of the complex global model (described in chapters *Motivation* and *Aim of modelling tool of precise diagnostics*). Results achieved on the level of local models could be generalized to formulate global model of cardiovascular system haemodynamics in men, which should improve understanding of function of heart and blood vessels as a whole. The global model also allows better interpretation of results of non invasive investigation of cardiovascular system as echocardiography, Doppler flowmetry and so on.
- Blood flow modelling in moving with peristaltic wave coordinates system causes simplifying because the problem becomes stationary.

- Hughes–Franc method allows us to avoid the stability problem connected with Stokes model, which is weakly stabilized with classical Galerkin approach. Another advantage of the Hughes–Franc method is a rigorous proof of existence and convergence.
- The implementation of the application which performs Hughes–Franc method has been made according to open paradigm of object-oriented programming, which allows us to modify the application easily and gives possibilities of an easy passage from Newtonian to non-Newtonian model.
- The problem is very sensitive to the pressure boundary values. The pressure boundary condition established on the basis of medical measurements, contains the average value of the pressure calculated over each tube cross-section, $p = g$ on $\partial\Omega$. There is a possibility that the pressure values closer to the real one may improve precision of the numerical solution.

REFERENCES

[1] I. Babuška. Error-bounds for finite element method. *Numer. Math.*, **16**: 322–333, 1969.
[2] I. Babuška. The finite element method with Lagrangian multipliers. *Numer. Math.*, **20**: 179–192, 1973.
[3] R. Berne, M. Levy. *Physiology.* The C.V. Mosby Company, St.Louis, Toronto, 1983.
[4] C.G. Caro, T.J. Pedley, R.C. Schroter, W.A Seed. *The Mechanics of the Circulation.* Oxford University Press, Oxford, 1978.
[5] M. Danielewski, B. Bożek, K. Holly, G. Myśliwiec, J. Sipowicz, R. Schaefer. Distributed simulation strategies of graphite electrode forming process. *Proc. of The Conf. Vecpar'98*, Porto, 1998.
[6] Y.C. Fung. *Biomechanics.* Springer-Verlag, New York, 1984.
[7] R.F. Furchgott, J.V. Zawadzki. The obligatory role of endothelial cells on the relaxation of arterial smooth muscle by acetylcholine. *Nature*, **288**: 373–376, 1980.
[8] S.M. Hilton. A peripheral arterial conduction mechanism underlying dilation of the femoral artery and concerned in functional vasodilation in skeletal muscle. *J Physiol.*, **149**: 93–111, 1959.
[9] M. Hoffman, J. Korewicki, Z. Zurzycki. *Serce Niewydolne.* Wyd. Medyczne, Warszawa, 1994.
[10] J. Holtz, U. Forstermann, U. Pohl, M. Geisler, E. Bassenge. Flow-dependent endothelium-mediated dilation of epicardial coronary arteries in conscious dogs: Effects of cyclo-oxygenase inhibition. *J. Cardiovasc. Pharmacol.*, **6**: 1161–1169, 1984.
[11] T.J.R. Hughes, L.P. Franca. Stabilized Finite Element Methods for the Stokes Problem. In: *Incompressible Computational Fluid Dynamics – Trends and Advances.* Cambridge University Press, 1991.
[12] J.A. Jensen. *Estimation of Blood Viscosities using Ultrasound.* Cambridge University Press, Cambridge, 1996.
[13] J. Kocemba, W. Król, K. Moczurad. Badania epidemiologiczne. *Folia Med. Cracov*, **18**: 509, 1976.
[14] T.W. Latham. *Fluid Motions in the Peristaltic Pump*, M.S. Thesis. Masachusetts Institute of Technology, 1966.
[15] M. Lie, O.M. Sjersted, F. Kill. Local regulation of vascular cross section during changes in femoral arterial blood flow in dogs. *Circ. Res.*, **27**: 727–737, 1970.
[16] R.L. Memmler, D.L. Wood. *Structure and Function of the Human Body.* J.B. Lippincott Company, Philadelphia, 1987.
[17] R.M. Nerem, W.A. Seed. An in vivo study of aortic flow disturbances. *Cardiovascular Research*, **6**: 1–14, 1972.
[18] R.M. Nerem, W.A. Seed, N.B. Wood. A study of the velocity distribution and transition to turbulence in the aorta. *J. Fluid Mech.*, **52**(1): 137–160, 1972.
[19] W.W. Nichols, M.F. O'Rourke. *McDonald's Blood Flow in Arteries*, 3rd edn. London, Edward Arnold, 1990.
[20] A. Nowicki. *Podstawy Ultrasonografii Dopplerowskiej.* Warszawa, PWN, 1995.
[21] M.F. O'Rourke. *Arterial Function in Health and Disease.* Edinburgh, Churchil Livingstone, 1982.
[22] U. Pohl, J. Holtz, R. Busse, E. Bassenge. Crucial role of the endothelium in the vasodilator response to increase flow in vivo. *Hypertension*, **8**: 37–44, 1986.
[23] G.M. Rubanyi, J.C. Romero, P.M. Vanhoutte. Flow-induced release of endothelium derived relaxing factor. *Am. J. Physiol*, **250**: H1145–1149, 1986.
[24] W.A. Seed, N.B. Wood. Velocity patterns in the aorta. *Cardiovascular Research*, **5**: 319–330, 1971.
[25] R. Schaefer, J. Krok, P. Leżański, J. Orkisz, P. Przybylski. Basic concepts of an open distributed system for cooperative design and structure analysis. *CAMES*, **3**: 169–186, 1996.
[26] A.H. Shapiro, M.Y. Jaffrin, S.L. Wienberg. Peristaltic pumping with long wavelength at low Reynolds number. *J. Fluid Mech.*, **37**(4): 799–825, 1969.
[27] J.B. Shukla, R.S. Parihar, B.R.P. Rao, S.P. Gupta. Effects of peripheral layer viscosity on peristaltic transport of a bio-fluid. *J. Fluid Mech.*, **97**(2): 225–237, 1980.
[28] V.P. Srivastava, M. Saxena. A two-fluid model of non-Newtonian blood flow induced by peristaltic waves. *Rheol. Acta*, **34**: 406–414, 1995.
[29] R. Temam. *Navier–Stokes Equations Theory and Numerical Analysis.* North-Holland, 1979.